

Isothermal titration calorimetry in a polymeric microdevice

Yuan Jia¹ · Zhixing Zhang¹ · Chao Su¹ · Qiao Lin¹

Received: 15 November 2016 / Accepted: 22 April 2017 / Published online: 28 April 2017
© Springer-Verlag Berlin Heidelberg 2017

Abstract Microelectromechanical systems (MEMS) technology can enable the integration of isothermal titration calorimetry (ITC) on a single chip for direct thermodynamic characterization. However, existing ITC microdevices either do not yet allow proper control of reaction conditions for thermodynamic characterization of biomolecular reaction systems or do not yet suitable for practical applications because of a lack of reliability, high costs, and other issues. This paper aims to address these limitations with polymeric MEMS-based quantitative ITC measurements. The polymer-based ITC device design eliminates the use of silicon and exploits the low thermal conductivity of the polymer substrate to achieve thermal isolation of reaction samples in the absence of any complex or fragile freestanding structures. The low-cost availability of polymers and the elimination of the freestanding structures simplify the fabrication process, increase the fabrication yield, reduce the device cost, and improve the device reliability. During the ITC device operation, reactants and reference solutions are introduced to their respective measurement chambers, and the reaction-induced differential thermal power is measured and used to compute the thermodynamic binding

parameters associated with the reaction. The potential utility of the device has been demonstrated with quantitative ITC measurements of a model reaction system in which the ligand BaCl₂ is titrated into the receptor 18-C-6 at a concentration of 2 mM.

Keywords Isothermal titration calorimetry (ITC) · Polymeric microdevice · Thermodynamic characterization · Biomolecular reactions systems

1 Introduction

Isothermal titration calorimetry (ITC) measures heat either released or absorbed when a ligand solution is titrated or added into a receptor solution of interest under isothermal conditions (Leavitt and Freire 2001). ITC is known to be the only technique that can simultaneously determine all reaction associated binding parameters in a single experiment and is label free and solution based, requiring no molecular labeling or surface immobilization (Malvern 2017). While widely used in basic biochemical studies as well as practical applications such as drug discovery and biotherapeutics development, conventional ITC instruments are limited by high cost, complicated design and construction, low throughput, and slow response times.

Microelectromechanical systems (MEMS) technology can enable the integration of ITC measurements on a single chip. However, MEMS devices that offer ITC capabilities do not yet allow proper control of reaction conditions for thermodynamic characterization of biomolecular reaction systems. In particular, flow-through-based MEMS calorimetric devices have limited sensitivity due to poor thermal isolation (Hany et al. 2010). In addition, devices that use droplet-based reactions

This article is part of the topical collection “2016 International Conference of Microfluidics, Nanofluidics and Lab-on-a-Chip, Dalian, China” guest edited by Chun Yang, Carolyn Ren and Xiangchun Xuan.

Electronic supplementary material The online version of this article (doi:10.1007/s10404-017-1925-4) contains supplementary material, which is available to authorized users.

✉ Qiao Lin
qlin@columbia.edu

¹ Department of Mechanical Engineering, Columbia University, New York, NY 10027, USA

generally do not allow for well-defined reaction volumes and are further complicated by evaporation-induced noise and volume change (Recht et al. 2008; Lubbers and Baudenbacher 2011; Xu et al. 2008). Hence, such devices are not well suited to quantitative measurement of thermodynamic reaction parameters.

To address these issues, our research group previously reported a closed-chamber-based MEMS ITC device that featured freestanding microfabricated differential calorimetric sensors, well-defined reaction volumes, and integrated micromixing capabilities (Wang et al. 2016). The silicon-based device showed potential for quantitative thermodynamic characterization, although several limitations were observed. First, the high thermal conductivity of silicon necessitated the use of complex and fragile freestanding structures (Mouaziz et al. 2006) to enhance device thermal isolation. This reduced yield caused significant reliability issues during the device's ITC operation and maintenance (e.g., cleaning) and made the device rather expensive to use. Second, the device also neglected the residue fluid flow effects and used a relatively high Reynolds number flow (~ 23) in the mixing channel. This resulted in significant noise that led to a relatively high limit of detection (650 nW). Hence, ITC measurements required a relatively high receptor concentration (5 mM for 18-C-6), which was not yet adequate for practical applications.

In this paper, we aim to address the limitations of existing MEMS ITC devices with polymeric MEMS-based quantitative measurements. The polymer-based ITC device design eliminates the use of silicon and exploits the low thermal conductivity of the polymer substrate to achieve thermal isolation of reaction samples in the absence of any complex or fragile freestanding structures. The use of inexpensive polymers and the elimination of the freestanding structures simplify the fabrication process, increase the fabrication yield, reduce the device cost, and improve the device reliability. In addition, the closed volume-based MEMS ITC approach, as initially demonstrated by the silicon-based device without further analysis, was systematically characterized in the present work to identify factors such as volume mismatch, reaction volume information, evaporation of reactants, and thermal activity in the mixing and transport of reactants before they enter the calorimetric chamber that influence the sensitivity and accuracy of ITC measurements. These insights are used to generate a polymer-based MEMS ITC design for more sensitive and reliable ITC measurements. The potential utility of the device is demonstrated with quantitative ITC measurements of a model reaction system in which the ligand BaCl_2 is titrated into the receptor 18-C-6 at a concentration of 2 mM.

2 Principle and design

In an ITC experiment for the characterization of a ligand–receptor system, the ligand with known concentration and volume is titrated or added into a known concentration of a receptor solution. From measurements during the titrations, the reaction heat is obtained as a function of the ligand concentration. For example, consider a biochemical binding system in which a receptor (M) and a ligand (X) bind in equilibrium and form the complex $M_\alpha X_\beta$:



where α , β are the stoichiometric coefficients of the receptor and of the ligand, respectively. The binding parameters of the system, which include the molar enthalpy change of binding (ΔH), the reaction stoichiometry ($N = \beta/\alpha$), as well as the reaction binding constant K_b , can thus be determined using the following binding equation, in which biological reaction heat Q is expressed as (MicroCal 2004):

$$Q = \frac{NM_t \Delta H V_0}{2} \left[1 + \frac{r}{N} + \frac{1}{NK_b M_t} - \sqrt{\left(1 + \frac{r}{N} + \frac{1}{NK_b M_t} \right)^2 - \frac{4r}{N}} \right] \quad (2)$$

and is a function of the ligand–receptor molar ratio (r). In the equation, M_t is the total concentration of the receptor (both free and bound) in the reaction volume V_0 , and X_t is the total concentration of the titrated ligand. The values of N , K_b , and ΔH are then determined by fitting to Eq. (2) using nonlinear least-squares analysis (Velazquez-Campoy et al. 2004).

In our approach to ITC measurements, the reaction heat is determined using a differential scheme, where the reaction and reference chambers are used for measuring heat in the presence (ligand–receptor system) and absence of the receptor (ligand–buffer system), respectively. Before entering their respective chamber, a series of liquid segments of different concentration of ligand in a constant volume at a controlled temperature are allowed to react with the same volume of the receptor and a pure buffer, respectively. The differential power generated (i.e., the thermal power difference between the reaction and reference chambers) can be represented as $\Delta P = P_s - P_r$, where P_s and P_r are the thermal power in the reaction and reference chambers, respectively. This differential power can be determined by:

$$\Delta P = \frac{\Delta U}{S} \quad (3)$$

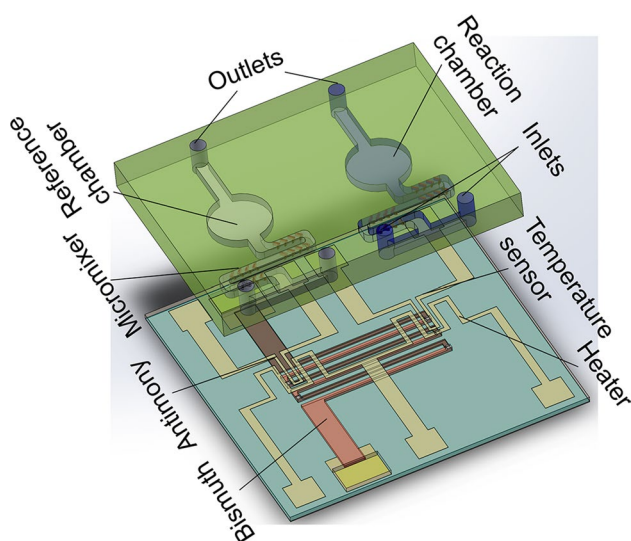


Fig. 1 Exposed view of the polymeric ITC microdevice. To clearly show the Sb-Bi thermopile, only five representative Sb-Bi thermopile junctions are included in the figure

where ΔU is the output of the thermopile and S is the device's responsivity, i.e., the output electrical voltage generated by unit differential thermal power (Wang and Lin 2012). The total heat released or absorbed Q_{total} in the calorimetric cell on each injection of reagent is determined by integrating the differential power generated over time. The biochemical reaction heat Q is then obtained by subtracting the non-specific heating contributions obtained from the negative control experiment.

Our ITC microdevice (Fig. 1) consists of two microfluidic chambers that are made from polydimethylsiloxane (PDMS). The chambers contain the binding system and a reference system, respectively. Each of the microchambers is situated on a polymeric substrate and surrounded by air cavities embedded in the sidewalls for effective thermal isolation. The serpentine flow channels connected to the chambers are each integrated with a passive chaotic micromixer that uses herringbone-shaped ridges in the ceiling of the channels to generate a chaotic flow pattern that induces mixing of the incoming liquid streams (Stroock et al. 2002). An antimony (Sb)-bismuth (Bi) thermopile (60 junctions) is patterned on the substrate and is aligned so that its hot and cold junctions are located beneath the chamber centers. Thin-film resistive microtemperature sensors and microheaters which are used for in situ monitoring of the chamber temperature, as well as for on-chip device calibration, are also integrated, on the substrate beneath the chambers' center. The thin-film resistive sensors and heaters are electrically isolated from the thermopile by a spin-coated polyimide passivation layer.

3 Experimental procedure

When performing ITC experiments using our approach, buffer and ligand solutions were first introduced into both the reaction and reference chambers, and the resulted differential voltage measured by the thermopile was recorded and used as a baseline, which also served as the negative control for the overall ITC measurements. Next, during the ITC measurements of ligand–receptor binding, a known concentration of receptor and different concentrations of ligand, which were typically in pure form and dissolved in well-conditioned buffer, were mixed in the micromixer and then entered the sample chamber. Simultaneously, the same concentrations of ligand and the buffer were also introduced, becoming mixed before entering the reference chamber. The differential thermal power between the chambers was determined from heat-induced differential voltage that was measured by the Sb-Bi thermopile and was used to compute the biochemical reaction heat Q .

Finally, the titration-enabling fluidic delivery was achieved by the following steps. First, air-separated segments of the same concentration of receptor and different concentrations of ligand solutions were each preloaded using a syringe pump into a Teflon access tubing. Titration of the ligand into the receptor (Fig. S1b) was achieved via merging the solutions segments in the micromixer and delivering into the reaction chamber. The ligand–receptor molar ratios were varied from merging different solutions segments that contain corresponding ligand and receptor concentrations. Similarly, two other access tubings were loaded with segments of ligand and buffer solutions, respectively. Similarly, solution segments of ligand and buffer were merged in the micromixer and delivered to the reference chamber. The preloading of the solution to the access tubings (four in total) and the subsequent delivering of the reagents to the appropriate measurement chambers were synchronized by a multiple-injection syringe pump (KD Scientific, KDS 220). Pure buffer solution and sterile water were also loaded between the reactant segments to clean the chambers.

4 Results and discussion

The closed-chamber-based MEMS ITC approach was systematically characterized in the present work to identify factors such as volume mismatch, reaction volume information, evaporation of reactants, and thermal activity in the mixing and transport of reactants before they enter the calorimetric chamber that influence the sensitivity and accuracy of ITC measurements. First, volume difference between the reaction and reference chambers was experimentally determined, and its effect on the steady-state response of the microdevice due to an input thermal

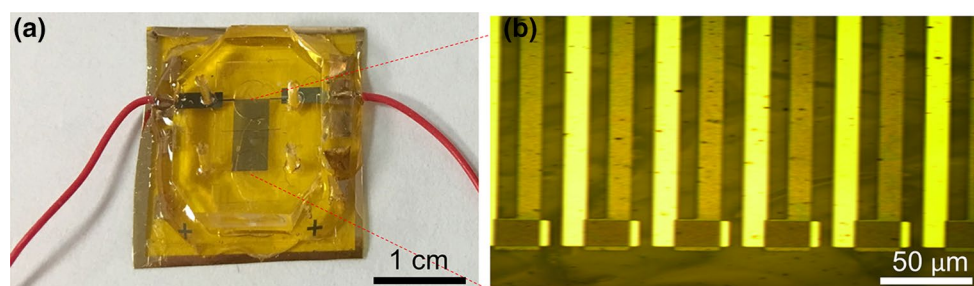


Fig. 2 **a** Fabricated polymeric ITC microdevice; **b** Sb-Bi thermopile junctions

power was characterized using numerical simulation. Next, the reaction volume information, the efficiency of the passive chaotic mixers, and the residence time of the reactants in the mixer and connecting channel were also investigated numerically. In addition, the microdevice characteristics, including the device responsivity, thermal time response and the device baseline noise, were characterized experimentally. Finally, the fully characterized microdevice was then used in quantitative ITC measurements of BaCl_2 reacting with 18-C-6. The ITC microdevice (Fig. 2a) used in the following experiments and simulation model had a 60-junction Sb-Bi thermopile (Fig. 2b) and a reaction and reference chamber with the same radius of 1286 μm and a height of 164, 155 μm , respectively. The center of the chambers was separated by 4.5 mm. The herringbone-shaped ridges integrated micromixers (width 200 μm , total length 15 mm) led the introduced solutions to the measurement chambers, while the solutions became well-mixed along the way. The herringbone-shaped ridges were placed on the ceiling of the microchannel, and each of them had a width of 40 μm , a height of 50 μm , a 30 μm separation distance between each other and formed a 60° with the channel sidewall.

4.1 Effects of volume mismatch

The first potential factor that may affect the sensitivity and accuracy of the microdevice is the volume mismatch between the reaction and reference chambers. To characterize this mismatch, the volume of the SU-8 mold, which was used in soft lithography to produce the reaction and reference microstructures, was determined (details included in SI) to have an average radius of 1287, 1286 μm , and an average chamber thickness of 163, 157 μm with a standard deviation of 5.35, 5.57 μm , respectively. The relatively large thickness standard deviation was expected due to the spinning of highly viscous SU-8 2150 solution, which after baking was thicker close to the edge of the wafer. Thus, an average of 5.6% volume difference was obtained for reaction and reference chambers.

Using COMSOL Multiphysics, we simulated two cases of the temperature distribution of the microdevice to characterize the effects of the volumetric difference between the calorimetric chambers. The simulation was performed in the absence of liquid flow, as the calorimetric measurements were performed after the liquid flow had been stopped. Also, any residual effect of the liquid flow was addressed by subtracting the baseline (Fig. 6) from the titration calorimetric measurement data. The first case considered a three-dimensional model of the ITC microdevice that included water-filled PDMS reaction and reference microstructures, thermopile junctions, Kapton substrate, passivation layers, and the polyimide-PDMS blend adhesive layer in between. The model accounts for the heat conduction inside the device and convection from the device's outer surfaces to the ambient (details are included in SI). The thickness of the reference microfluidic structures was intentionally reduced by 5.6% to account for the volume difference due to fabrication tolerances. In addition, because the binding reagents were homogenous, a thermal power of 1.63 μW (obtained based on empirical 18-C-6 and BaCl_2 reaction data) was applied uniformly in the reaction chamber to represent typical 18-C-6 and BaCl_2 reaction heat generation. From the simulation, an average thermopile differential temperature of 6.38×10^{-4} K (Fig. 3a) was obtained. Next, the second case considered the same microdevice model; however, in this case, the reaction and reference microstructures had identical dimensions. When the same power was applied to the reaction chamber, an average thermopile differential temperature of 6.31×10^{-4} K was obtained (Fig. 3b) between the reaction and reference measurement chambers. Thus, the differential temperature from these two models differed by 1.1%, which was considered insignificant so that the effect of volumetric difference on the steady-state device response was negligible.

4.2 Determination of the reaction volume information

Another potential source of error in determining the reaction binding parameters was the inaccurate reaction volume information. During ITC measurements, besides

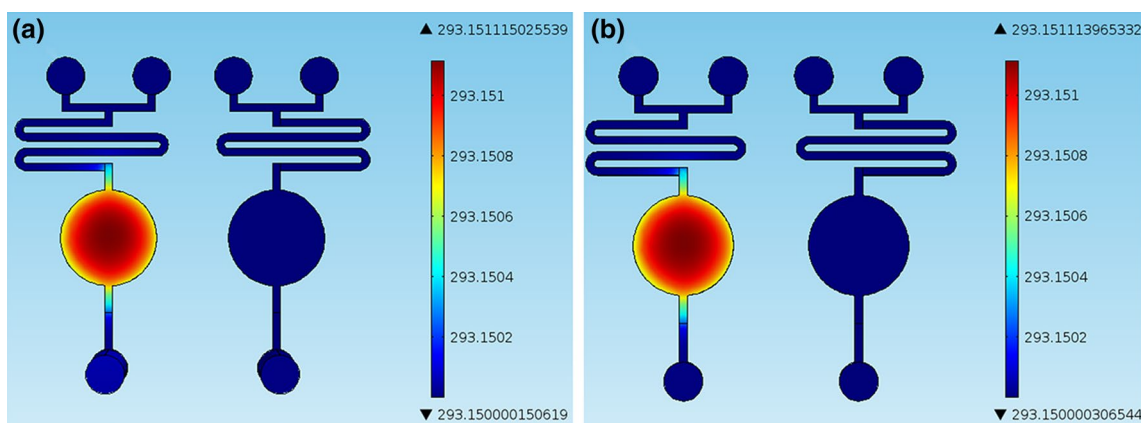


Fig. 3 Microdevice temperature distribution when a unit power density is applied to the reaction chamber: **a** model with a 5.6% reaction/reference microfluidic structures volume difference; **b** model with no volume difference

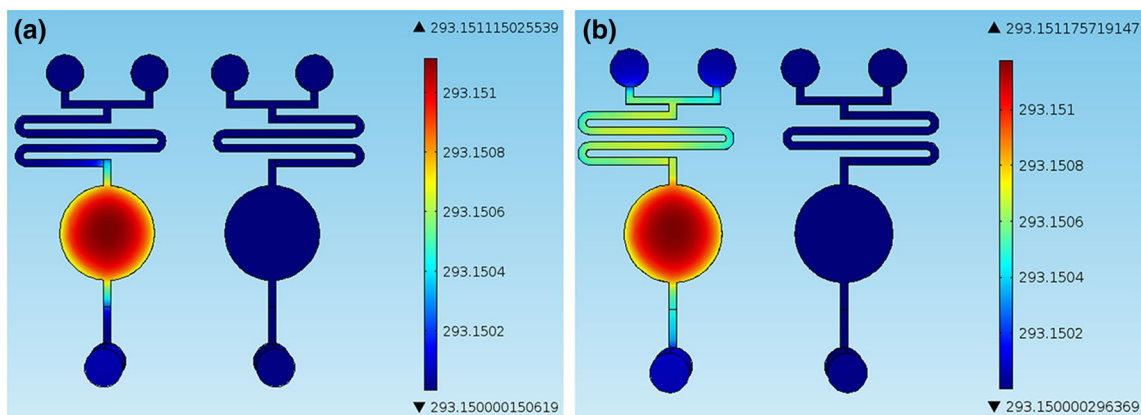


Fig. 4 Differential temperature between the reaction and reference chambers. **a** A uniform thermal power was applied to the reaction chamber; **b** the uniform thermal power of the same density was applied to chamber and associated microfluidic components

the reaction chamber, binding reaction would also have occurred in other microfluidic structures such as the mixing channels and channel leading into the outlet, contributing to the total heat generation. We used simulation to assess the appropriateness of the reaction chamber volume to be used as the reaction volume in the computation of thermodynamic properties. In the simulation, we first computed the differential temperature when a uniform thermal power was applied to the reaction chamber alone (Fig. 4a). Then, a uniform thermal power of the same density was applied to the reaction chamber and its associated microfluidic components including the micromixer and the connection channels) to conservative estimate the effects of different choices of the reaction volume (Fig. 4b). The differential temperature in these two cases differed only by 7%. Thus, it was determined that it was acceptable to use the reaction chamber volume to compute the thermodynamic properties of the reaction system.

4.3 Characterization of reagents mixing

Next, to further understand the behavior of the reagents streams passing through the micromixer and to demonstrate that the reagents had become fully mixed before entering their perspective measurement chambers, this section presented a numeric simulation of a chaotic micromixer embedded in a serpentine channel that considered the interactions of the fluid flow and the passive chaotic micromixer. The results would yield insight into the design of microchannel dimensions, especially the length of the flow channel. Additionally, the mixing efficiency at the outlet of the passive chaotic mixer incorporated channel was determined and compared with the mixing efficiency of a bare PDMS channel (details included in SI). As a result, the distribution of the solute concentration in the channel is shown in Fig. 5a, b. For the mixer-embedded channel, as the fluid stream flowing

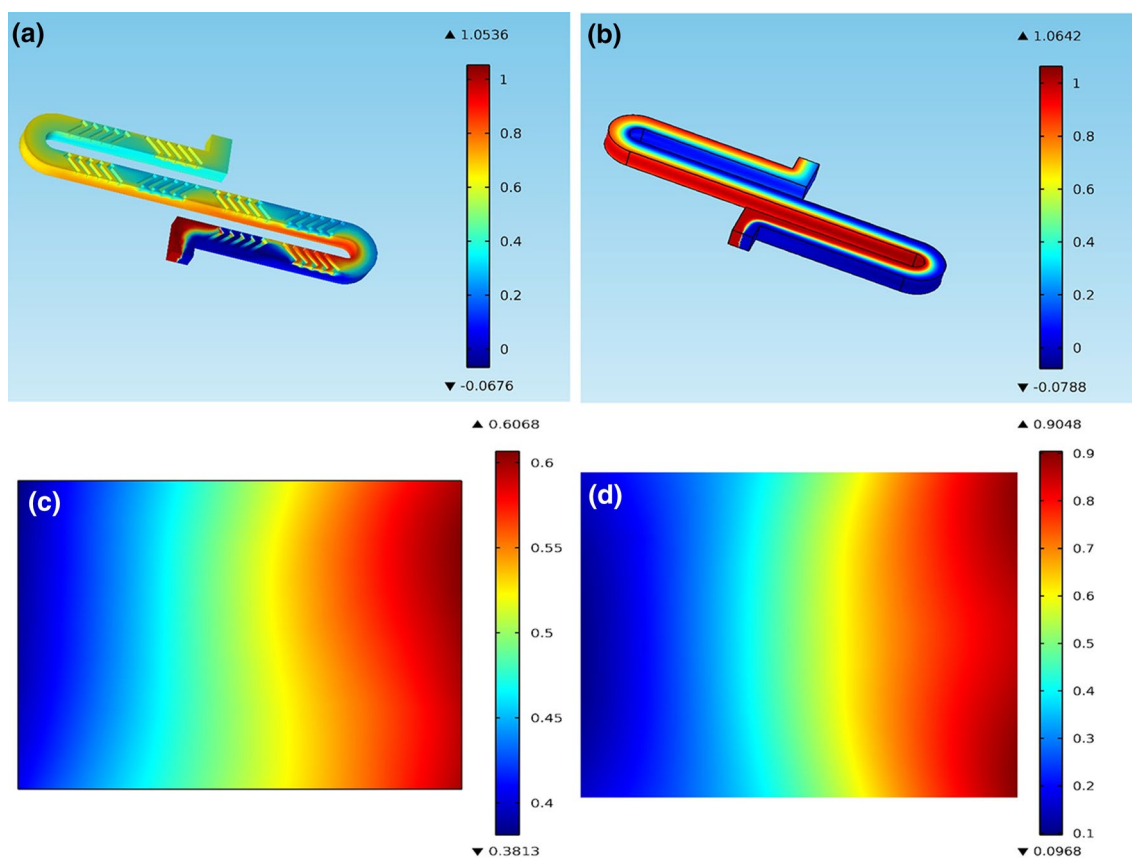


Fig. 5 Mixing effectiveness of **a** a chaotic mixer integrated channel versus **b** a straight channel; **c** solute concentration gradient at the outlet of the chaotic mixer integrated channel; **d** solute concentration

gradient at the outlet of the straight channel. The simulations presented here were performed in separate serpentine mixing channels as the mixing was not affected by the rest of the microdevice

through the channel, the solute concentration gradient prescribed by the initial condition gradually decreases, which was evident by the disappearance of the concentration interface at the end of the channel. On the contrary, for the same channel length, a still rather large concentration gradient existed at the outlet of the bare PDMS channel. The solute concentration distribution at the outlet of both channels (Fig. 5c, d) was used to quantify the mixing uniformity. Calculating using the standard definition (Feng et al. 2013), a mixing uniformity of 92 and 73% is obtained for the flow channels of 15 mm in length with and without the chaotic mixer, respectively. In addition, the mixing time was defined as the time required for the reagents to achieve a 90% mixing efficiency; therefore, using a combined flowrate of 50 $\mu\text{L}/\text{min}$, it would take 570 ms for reagents to travel from the beginning to the end of the micromixer. The device was then considered suitable to characterize the thermodynamic binding parameters of a reaction that have a time scale sufficiently slower than the mixing time to avoid heat loss in the micromixer.

4.4 ITC microdevice characteristics

We next investigated a set of device characteristics that are important to quantitative ITC measurements, including the reagent loss rate through permeation, device responsivity, thermal time response, and stability of the baseline. First, as we employed a closed-chamber design (compared to the open-volume design of the droplet-based calorimeters), any evaporative reagent loss would occur only through the PDMS walls. Using available empirical data on water permeation through PDMS (SABIC 2017), the reagent loss rate was estimated to be approximately 2% of the reagent volume per hour (Lamberti et al. 2014). Since the entire ITC experiment was completed within 30 min, the reagent loss in our ITC microdevice was negligibly small. Next, experiment (detail included in SI) was carried out to determine the steady-state response of the device, i.e., the device responsivity. At 298 K, the steady-state response of the ITC device was found to depend on the differential power in a highly linear manner, yielding an approximately constant responsivity of $S = 3.7 \text{ mV}/\text{mW}$ (Fig. S2), which

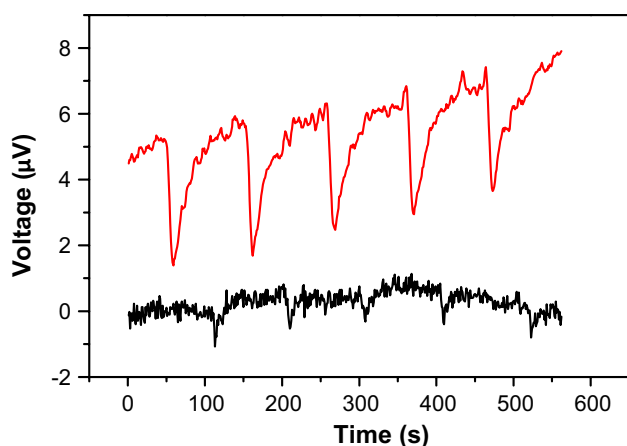


Fig. 6 Repeatable device output upon introduction of 2 mM 18-C-6 and 2 mM BaCl₂ compared with water baseline (baseline is intentionally shifted down)

was sufficient for measuring the heat evolved in our model reaction. We also characterized the device's responsivity at controlled ambient temperatures provided by the thermal enclosure from 20 to 45 °C and found that it remained constant with a relative standard deviation of less than 3%. Therefore, the temperature dependence of the device responsivity could thus be ignored. Next, a thermal time response of 2.6 s was obtained using the ITC microdevice (Fig. S3). It was considered appropriate for characterizing biomolecular reaction systems with kinetics that were sufficiently slow compared with this thermal response time.

Finally, the overall baseline of the measurement that also served as the negative control of the ITC experiment was measured by introducing sterile water and 0.4–5 mM BaCl₂ to both the reaction chamber and reference chamber simultaneously. To test the stability of this baseline, five sequential injections of the reagents were administered, each with a 2-min interval, and at a combined rate of 50 µL/min. All five measurements showed a flow residual non-reaction-specific peaks that were subtracted from the analysis. The baseline noise (~200 nW) also represented the detection limit of our ITC microdevice, which was considered typically adequate for measuring the thermal power generated in biomolecular reaction systems. To compare the baseline noise with the reaction heat-induced differential thermal power, 0.8 mM BaCl₂ and 2 mM 18-C-6 (each 0.4 µL) were mixed and introduced at the rate of 50 µL/min to the reaction chamber while the reference chamber was introduced with 0.8 mM BaCl₂ and water. Contrary to the baseline, the ITC microdevice exhibited a reaction-specific spike attributable to the exothermic nature of the binding between 18-C-6 and BaCl₂ (Fig. 6).

As a result, a repeatable signal-to-noise ratio of ~5 (appropriate for titration measurements) was observed.

Furthermore, it was important to note that the effects of thermal activity in the mixer and the connecting channel from the mixer to the calorimetric measurement chamber (Fig. 1) were determined by the residence time of the reactants in the mixer and connecting channel (referred to as the mixing and transport time) as compared to the reaction time, i.e., the scale due to reaction kinetics. In our measurements, the mixing and transport time (0.57 s, estimated based on the combined ligand and receptor carrier flow rate) was short compared to the reaction time [~10 s, estimated based on consideration of reaction kinetics (Burnouf et al. 2012)] for the system of 18-C-6 and BaCl₂. Hence, reaction and the associated thermal activity in the mixer and connecting channel can be neglected, and the thermal power measured by the thermopile can be accurately considered to be originated from the reaction of fully mixed reactants in the calorimetric chamber. For other reaction systems with reaction times dominated by the mixing and transport time, the thermal power due to reaction in the mixer and connecting channel cannot be neglected. Fortunately, as this thermal power is rapidly swept into the calorimetric chamber by the imposed fluid flow, measurements in the calorimetric chamber can still achieve adequate accuracy. For a conservative estimate, we considered the transport of a thermal power uniformly distributed in the channel. Based on convective heat transfer simulation in the mixer and connecting channel using the same flow rate (total of 50 µL/min), it was estimated that approximately 10% of this thermal power would be lost through the walls of the mixer and connecting channel before entering the calorimetric chamber. Thus, the measurement error can still be considered adequately small. More accurate measurements can be achieved by an improved microfluidic design. In particular, the reactants can be mixed and then allowed to react in the same location (i.e., by merging the mixer and the calorimetric chamber) to eliminate the unmeasured reaction thermal power, and such a design is being investigated in our ongoing work.

4.5 ITC measurements

The fully characterized microdevice was then used to perform ITC measurements of the titrated reaction of BaCl₂ with 18-C-6 to demonstrate its potential for thermodynamic characterization of the biomolecular reaction systems. At the controlled temperature of 298 K, titration reaction used a fixed receptor concentration of 18-C-6 (2 mM) and a series of different ligand concentrations of BaCl₂ (in the range of 0.4–5 mM), allowing the molar ratio of BaCl₂ to 18-C-6 to be varied from 0.2 to 2.5. Measurement of reaction at each molar ratio occurred in a duration of approximately 4 min (2-min test duration, with 2-min injection interval) with the entire ITC measurement

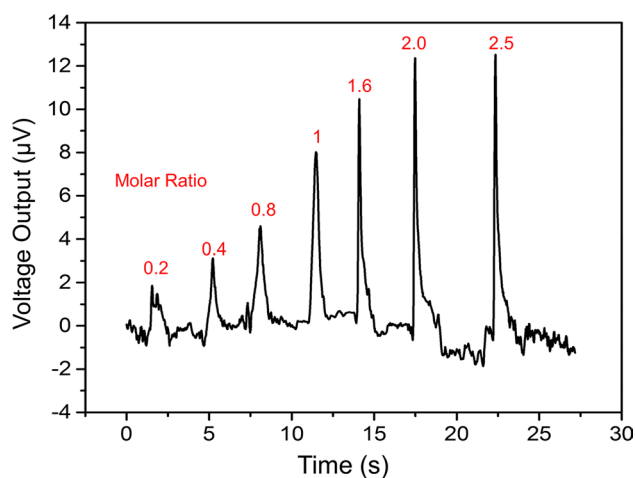


Fig. 7 Device output of the binding of 2 mM 18-C-6 and BaCl_2 at different molar ratios (indicated above each peak) at 298 K

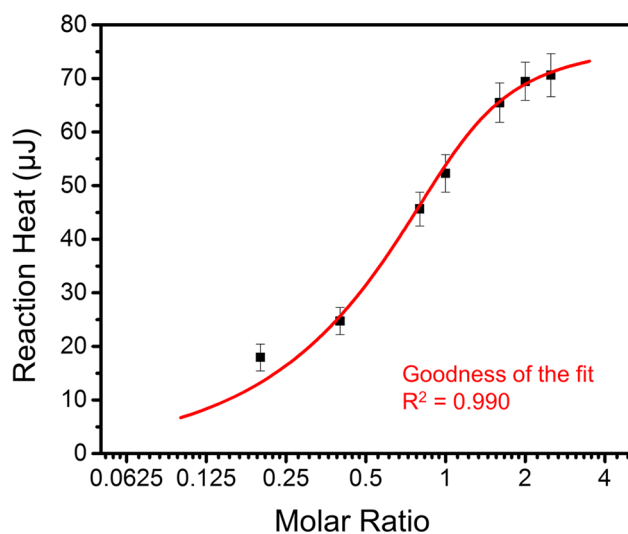


Fig. 8 Calculated the biochemical heat of 18-C-6 reacting with BaCl_2 at different molar ratios, and fitted curve to one binding-site model. *Error bars* represent the standard deviation calculated from at least three repeated measurements at each molar ratio

completed within approximately 28 min. The baseline-subtracted device output (Fig. 7) exhibited spikes consistent with the titration reactions. Each spike in the device output corresponded to each titration, with a magnitude increasing consistently with titration number. However, no device output increase was observed between the molar ratio of 2 and 2.5, indicating excessive ligand (BaCl_2) concentration at a molar ratio of 2.5, and the reaction was most likely saturated at a molar ratio of 2. This was expected for the reaction system.

Equation (3) was then used to calculate the differential thermal power that was induced by the titration reaction. The

reaction heat at each molar ratio was then determined by integrating the thermal power over the entire period of reaction. A thermodynamic binding isotherm (Fig. 8) was obtained by plotting the reaction heat as a function of the molar ratio (Wiseman et al. 1989). It could be seen that the reaction heat increased monotonically with the molar ratio until approaching saturation (molar ratio of 2) reflecting that the most binding sites of 18-C-6 were occupied with the addition of BaCl_2 until the binding sites were no longer available and excessive BaCl_2 became free ligand in solution.

The binding parameters of the reaction system were then determined from the least-square best-fit curve to the binding isotherm. The stoichiometry N , the equilibrium binding constant K_b , and the molar enthalpy change ΔH were determined to be 1.01, $5.5 \times 10^3 \text{ M}^{-1}$, and 32.0 kJ/mol at 298 K, respectively. These properties corresponded to the one to one binding of 18-C-6 and BaCl_2 and were within 5% difference with published data using conventional instruments (Mizoue and Tellinghuisen 2004).

5 Conclusions

We have described a polymeric MEMS-based quantitative measurements approach for the thermodynamic characterization of biomolecular reaction systems. The polymer-based ITC device design eliminates the use of silicon and exploits the low thermal conductivity of the polymer substrate to achieve thermal isolation of reaction samples in the absence of any complex or fragile freestanding structures. The low-cost availability of polymers and the elimination of the freestanding structures simplify the fabrication process, increase the fabrication yield, reduce the device cost, and improve the device reliability. The ITC microdevice consists of a pair of PDMS microfluidic structures for reactants and reference solutions to be introduced at a series of molar ratios mixed in a passive chaotic mixer, and fed into the calorimetric measurement chambers at controlled time duration. As the reaction occurs, the resulting differential thermal power between the reaction and reference chambers is measured using a thin-film Sb-Bi thermopile that is embedded in the chamber-supporting polymeric substrate.

The closed volume-based MEMS ITC approach was first systematically characterized in the present work to identify factors such as volume mismatch, reaction volume information, evaporation of reactants, and thermal activity in the mixing and transport of reactants before they entered the calorimetric chamber that influenced the sensitivity and accuracy of ITC measurements. The potential utility of the device was demonstrated with quantitative ITC measurements of a model reaction system in which the ligand BaCl_2 is titrated into the receptor

18-C-6 at a reduced concentration of 2 mM. At the controlled temperature of 298 K, the thermodynamic binding parameters of the reaction systems, including the stoichiometry, equilibrium binding constant, and enthalpy change, were obtained and found to agree with published data obtained using commercially available ITC instruments. These results demonstrate the potential of the microdevice for quantitative ITC characterization of biomolecular interactions.

Acknowledgements The authors would like to thank Timothy Olsen and Yu Zhao for their valuable comments.

References

- Burnouf D, Ennifar E, Guedich S, Puffer B, Hoffmann G, Bec G et al (2012) kinITC: a new method for obtaining joint thermodynamic and kinetic data by isothermal titration calorimetry. *J Am Chem Soc* 134:559–565
- Feng XS, Ren YK, Jiang HY (2013) An effective splitting-and-recombination micromixer with self-rotated contact surface for wide Reynolds number range applications. *Biomicrofluidics* 7(5):54121. doi:10.1063/1.4827598
- Hany C, Lebrun H, Pradere C, Toutain J, Batsale JC (2010) Thermal analysis of chemical reaction with a continuous microfluidic calorimeter. *Chem Eng J* 160:814–822
- Lamberti A, Marasso SL, Cocuzza M (2014) PDMS membranes with tunable gas permeability for microfluidic applications. *RSC Adv* 4:61415–61419
- Leavitt S, Freire E (2001) Direct measurement of protein binding energetics by isothermal titration calorimetry. *Curr Opin Struct Biol* 11:560–566
- Lubbers B, Baudenbacher F (2011) Isothermal titration calorimetry in nanoliter droplets with subsecond time constants. *Anal Chem* 83:7955–7961
- Malvern (2017) Isothermal titration calorimetry. <http://www.malvern.com>
- MicroCal (2004) ITC Data Analysis in Origin: Tutorial Guide
- Mizoue LS, Tellinghuisen J (2004) Calorimetric vs. van't Hoff binding enthalpies from isothermal titration calorimetry: Ba²⁺-crown ether complexation. *Biophys Chem* 110:15–24
- Mouazziz S, Boero G, Moresi G, Degen C, Lin Q, Meier B et al (2006) Combined Al-protection and HF-vapor release process for ultrathin single crystal silicon cantilevers. *Microelectron Eng* 83:1306–1308
- Recht MI, De Bruyker D, Bell AG, Wolkin MV, Peeters E, Anderson GB et al (2008) Enthalpy array analysis of enzymatic and binding reactions. *Anal Biochem* 377:33–39
- SABIC (2017) Innovative plastics, oxygen and water permeability. http://www.pod-sabic-ip.com/KBAM/Reflection/Assets/Thumbnail/10620_4.pdf
- Stroock AD, Dertinger SKW, Ajdari A, Mezić I, Stone HA, Whitesides GM (2002) Chaotic mixer for microchannels. *Science* 295:647–651
- Velazquez-Campoy A, Leavitt SA, Freire E (2004) Characterization of protein–protein interactions by isothermal titration calorimetry. In: Fu H (ed) *Protein–protein interactions: methods and applications*, Humana Press, Totowa, pp 35–54
- Wang B, Lin Q (2012) A MEMS differential-scanning-calorimetric sensor for thermodynamic characterization of biomolecules. *J Microelectromech Syst* 21:1165–1171
- Wang B, Jia Y, Lin Q (2016) A microfabrication-based approach to quantitative isothermal titration calorimetry. *Biosens Bioelectron* 78:438–446
- Wiseman T, Williston S, Brandts JF, Lin LN (1989) Rapid Measurement of binding constants and heats of binding using a new titration calorimeter. *Anal Biochem* 179:131–137
- Xu J, Reiserer R, Tellinghuisen J, Wikswo JP, Baudenbacher FJ (2008) A microfabricated nanocalorimeter: design, characterization, and chemical calibration. *Anal Chem* 80:2728–2733